Molybdic Acid-Functionalized Nano-Fe₃O₄@TiO₂ as a Novel and Magnetically Separable Catalyst for the Synthesis of Coumarin-Containing Sulfonamide Derivatives

Jamileh Etemad Gholtash, Mahnaz Farahi,* Bahador Karami and Mahsa Abdollahi

Department of Chemistry, Yasouj University, P. O. Box 353, Yasouj 75918-74831, Iran

* Corresponding author: E-mail: farahimb@yu.ac.ir

Abstract

Supported molybdic acid on nano-Fe₃O₄@TiO₂ (Fe₃O₄@TiO₂@(CH₂)₃OMoO₃H) has been successfully prepared, characterized and applied as a catalyst for the synthesis of sulfonamide containing coumarin moieties. The prepared Fe₃O₄ nanoparticles by coprecipitation of Fe^{2+} and Fe^{3+} ions were treated with tetraethyl orthotitanate to obtain Fe₃O₄@TiO₂. By anchoring 3-chloropropyltriethoxysilan on Fe₃O₄@TiO₂ followed by reacting with molybdic acid, the desired catalyst was produced. The synthesized catalyst was characterized using XRD, SEM, EDS, FT-IR and VSM analysis. Fe₃O₄@TiO₂@(CH₂)₃OMoO₃H was used as a catalyst for the synthesis of sulfonamide containing coumarin moieties *via* a three-component reaction of aryl aldehydes, *para*-toluenesulfonamide and 4-hydroxycoumarin or 5,7-dihydroxy-4-methylcoumarin. The catalyst recovery test showed the catalyst is highly reusable without losing its activity.

Keywords: Nanocatalyst; *para*-toluenesulfonamide; aromatic aldehydes; 4-hydroxycoumarin; 5,7-dihydroxy-4-methyl-coumarin

1. Introduction

Nanochemistry is becoming increasingly significant which involves the synthesis and application of nanoparticles of different sizes and shapes.[1–9] Nanoparticles are different from their bulk counterparts and show special properties. A considerable amount of attention to nanoparticles is due to their unique properties such as ease of availability, chemical inertness, high surface area to volume ratio, high activity and selectivity, thermal stability and low toxicity.[10,11] Nanomaterials have been widely utilized as solid support material for the design of environmentally benign heterogeneous catalysts to address various economic and green chemistry issues.[12–15] Among them, magnetic nanoparticles (MNPs), especially nano-Fe₃O₄, have been more desirable because of their remarkable advantages. Nano-Fe₃O₄ has been intensively used as catalytic supports owing to the capability of separation from the reaction mixture *via* an external magnet which achieves a simple separation without filtration.[16,17] Supported catalysts on nano-Fe₃O₄ show not only high catalytic activity but also a high degree of chemical stability and they do not swell in organic solvents.

Nano-TiO₂ owing to its nontoxicity, long-term photostability, and high effectiveness has broadly been applied as catalyst in many organic transformations.[18,19] It has good mechanical resistance and stability in acidic and oxidative environments. Nano-TiO₂ is broadly utilized in fuel processing because of its tunable porous surface and distribution, high thermal stability and mechanical strength.[20] Despite the several mentioned advantages of TiO₂ nanoparticles, they are difficult to separate from the reaction media beacause of their small size. To simplify the separation and in order to increase the surface area, TiO₂ can be immobilized on magnetic nanoparticles to produce magnetically recoverable heterogeneous catalysts.[21–23]

In recent years, there has been an increased interest on the utilization of sulfonamide derivatives as basic constituents of numerous drugs include anticancer, anti-inflammatory, antiviral agents and HIV-protease inhibitors.[24–26] Antibacterial agents with sulfonamide structure, *e.g.* sulfadiazine have been therapeutically used for many decades.[27] They

have also been applied as azo dyes for achieving improved light stability, water solubility, and fixation of fibers. Sulfonamides are also known as inhibitors of the activity of the enzymes, such as dihydropteroate synthase (DHPS), matrix metalloproteinase, and carbonic anhydrase (CA).[28]

Coumarins as a class of lactones are important heterocycles that not only have many biological activities, but are also found in the structure of a large number of natural compounds.[29] With an entirely looking at medicinally important heterocycles, we find numerous drugs containing coumarin moiety.[30–32] Their easy synthetic modifications cause the design and synthesis of various coumarin-based derivatives with diverse activities against cancer.[33] Also, coumarins are widely employed as cosmetics, pigments and agrochemicals. They can be fused with different classes of heterocycles to obtain novel useful compounds. The unique properties and wide applications of coumarins have promoted extensive studies for the synthesis of these heterocycles.

Due to these benefits and as a continuation of our studies on the preparation of new heterogeneous catalysts,[34–36] herein we have developed synthesis and characterization of $Fe_3O_4@TiO_2@(CH_2)_3OMoO_3H$ as a novel recoverable nanocatalyst. Then, its application was investigated for the synthesis of sulfonamide containing coumarin moieties.

2. Results and Discussion

Because of reasonable needs for clean and green heterogeneous catalysts, $Fe_3O_4@TiO_2@(CH_2)_3OMoO_3H$ was synthesized following the procedure shown in Scheme 1. In the first step, the magnetic Fe_3O_4 nanoparticles were synthesized by coprecipitation of iron(II) and iron(III) ions.[17] Consequently, the TiO_2 shell was prepared by the hydrolysis of tetraethyl orthotitanate (TEOT) in an absolute ethanol/acetonitrile mixture in the presence of the well-dispersed Fe_3O_4 nanocrystals.[37] In continuation, the OH groups on the titanium coating magnetic nanoparticles ($Fe_3O_4@TiO_2$) can be functionalized with 3-chloropropyltriethoxysilan molecule.[38] Next, the new catalyst **1** was obtained by replacing chloride group using molybdic acid. The structure of the nanocatalyst **1** was studied and fully characterized using SEM, EDX, VSM, XRD, and FT-IR.

Fig. 1 shows the wide-angle XRD patterns of nano-Fe_3O_4, $Fe_3O_4@TiO_2$ and $Fe_3O_4@TiO_2@(CH_2)_3OMoO_3H$. As shown in Figure 1a, all the peaks agreed on face-centered cubic (fcc) Fe_3O_4. The data showed diffraction peaks at $2\theta = 37.158, 43.173, 66.98, 74.188,$ and 79.171 which can be indexed to (222), (400), (442), (533), and (444) with the JCPD 01-88-0315. Additionally, the peak of the highest in-
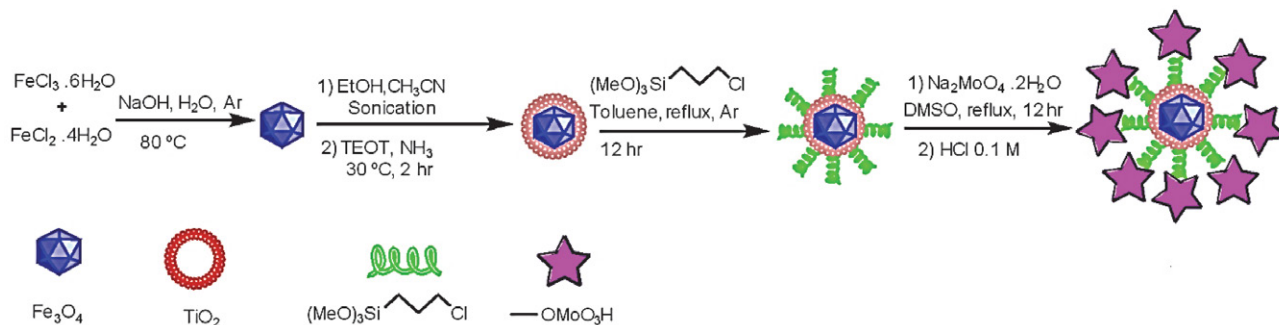
Scheme 1. Synthesis of $Fe_3O_4@TiO_2@(CH_2)_3OMoO_3H$ (**1**).
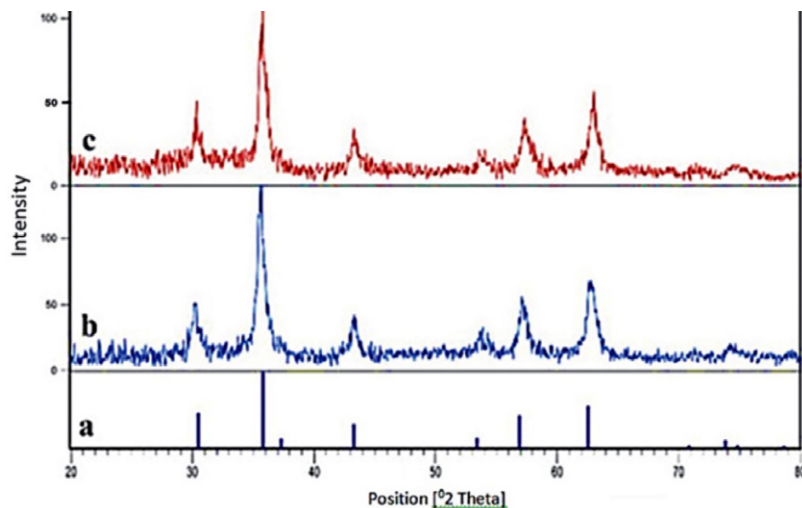
Figure 1. The XRD patterns of (a) nano-Fe_3O_4, (b) $Fe_3O_4@TiO_2$ and (c) $Fe_3O_4@TiO_2@(CH_2)_3OMoO_3H$.

tensity (311, $2\theta = 35.522$) was picked out to evaluate the particle diameter of the nanoparticles. Furthermore, in Figure 1b a broad diffraction peak appeared at $2\theta = 20$–30 nm that can be indexed to amorphous TiO_2.[39] The main peaks for the $Fe_3O_4@TiO_2$ are similar to the standard Fe_3O_4 particles, which reveals that the crystal structure of $Fe_3O_4@TiO_2$ is well coated. No obvious diffraction peak for the TiO_2 is observed, suggesting amorphous TiO_2 coating is formed by the hydrolysis of tetraethyl titanate (TEOT) in the presence of the well-dispersed Fe_3O_4 nano-crystals by a sol-gel process.[40] In Figure 1c, the confirming peak showing the presence of molybdate group has appeared in the range of $2\theta = 20$–$30°$ which is covered by the broad peak of TiO_2.[39, 41]

The FT-IR spectra of Fe_3O_4, $Fe_3O_4@TiO_2$, $Fe_3O_4@TiO_2@(CH_2)_3Cl$ and $Fe_3O_4@TiO_2@(CH_2)_3OMoO_3H$ were compared to analyze the progress of catalyst synthesis (Fig. 2). The observed characteristic peaks due to Fe–O stretching vibration at 583 cm^{-1} in all compared spectra is a confirmation of which nanostructure of Fe_3O_4 is preserved during the process. The appeared peaks at 1118 and 1400 cm^{-1} in Fig. 2b could be associated with stretching vibration modes of Ti–O and Fe–O–Ti bonds, respectively.[35] In Fig. 2c, the CH_2 bending as broadband and symmetric CH_2 and asymmetric CH_2 of the alkyl chains appear at 1480 cm^{-1} and 2860–2923 cm^{-1}, respectively. Fig. 2d shows new bands at 1623 and 3297–3436 cm^{-1} attributable to stretching vibration of Mo–O and OH.[43,44]

The vibrating sample magnetometer (VSM) was applied to evaluate the magnetic measurement of the prepared catalyst (Fig. 3). Based on the results, the saturation magnetization for $Fe_3O_4@TiO_2@(CH_2)_3OMoO_3H$ and $Fe_3O_4@TiO_2$ are 22.98 and 77.85 emu g^{-1}, respectively. The decrease of the saturation magnetization of $Fe_3O_4@TiO_2$

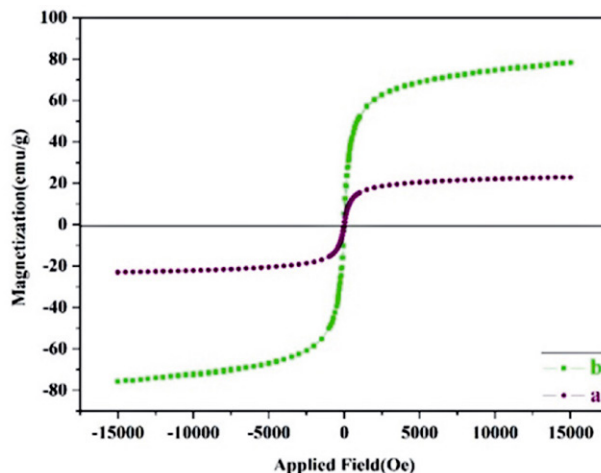**Figure 3.** Room-temperature magnetization curves of (a) $Fe_3O_4@TiO_2@(CH_2)_3OMoO_3H$ and (b) $Fe_3O_4@TiO_2$.

after surface coating with molybdic acid was ascribed to the increase of particle size of $Fe_3O_4@TiO_2$. This evidence indicates that molybdic acid immobilized on modified TiO_2-coated Fe_3O_4 has been successfully obtained.

The surface morphology of $Fe_3O_4@TiO_2@(CH_2)_3O$-MoO_3H was observed *via* a scanning electron microscopy (Fig. 4). The result demonstrates that nearly spherical nanoparticles with a narrow distribution were obtained with an average diameter of about 43.25 nm. Energy-dispersive X-ray spectroscopy (EDS) analysis of $Fe_3O_4@TiO_2@(CH_2)_3OMoO_3H$ (Fig. 5) contains all expected elemental cases including Fe, Ti, Mo, C, Si and O. The EDS spectra of the catalyst confirmed the existence of molybdate and hence indicated that molybdic acid grafted successfully on the catalyst surface.
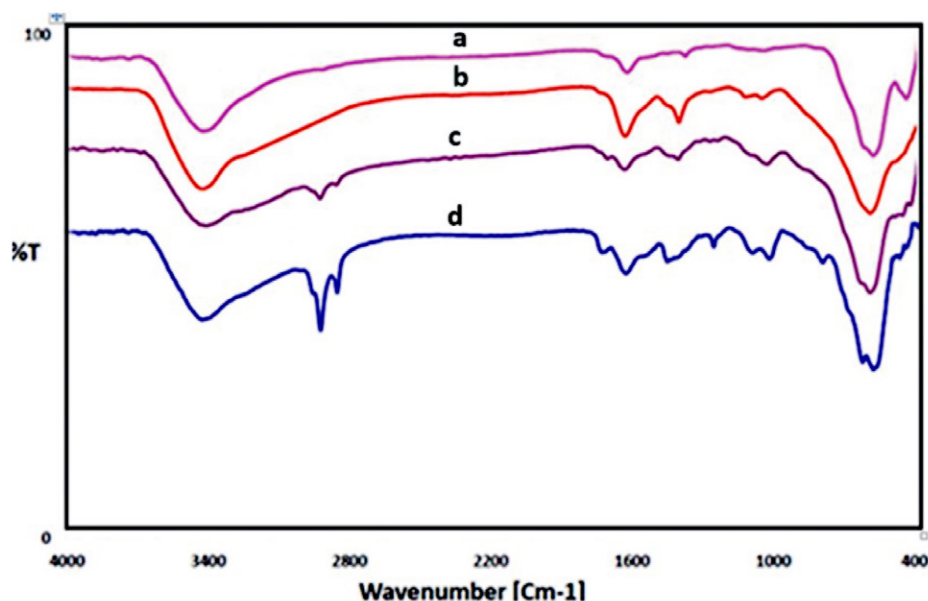

Figure 2. The FT-IR spectra of (a) Fe_3O_4, (b) $Fe_3O_4@TiO_2$, (c) $Fe_3O_4@TiO_2@(CH_2)_3Cl$, and (d) $Fe_3O_4@TiO_2@(CH_2)_3OMo_3H$.
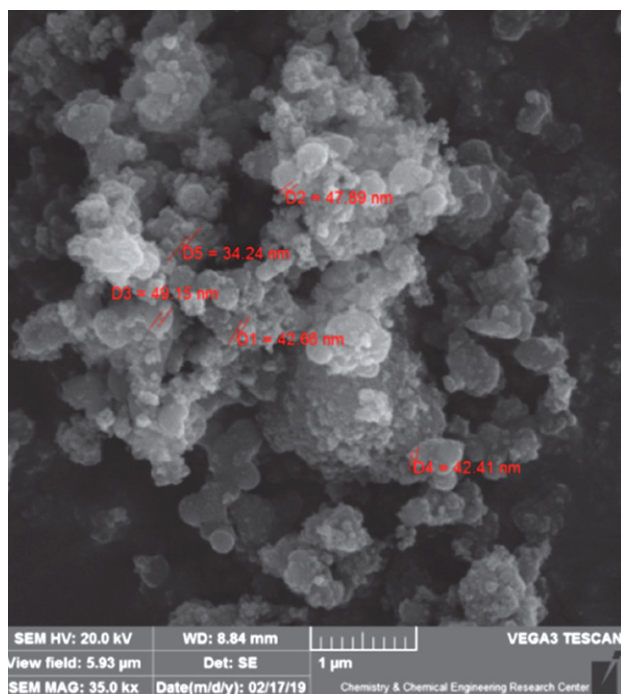
Figure 4. The SEM imag of $Fe_3O_4@TiO_2@(CH_2)_3OMoO_3H$.
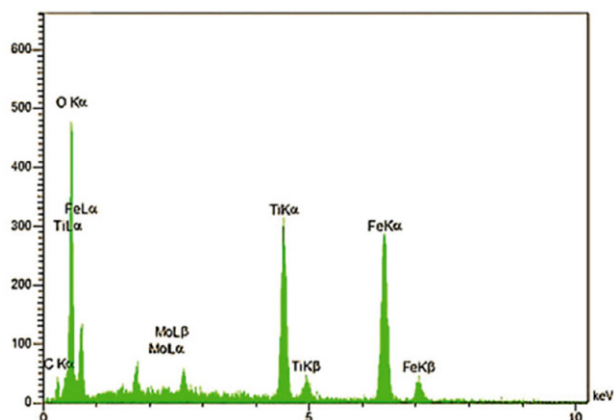
Figure 5. EDS analysis of $Fe_3O_4@TiO_2@(CH_2)_3OMoO_3H$.

The catalytic activity of $Fe_3O_4@TiO_2@(CH_2)_3O-MoO_3H$ was investigated in the synthesis of sulfonamide containing coumarins **6** *via* the reaction of aryl aldehydes (**2**), *para*-toluenesulfonamide (**3**) and compound **5** (4-hydroxycoumarin or 5,7-dihydroxy-4-methylcoumarin) (Scheme 2).
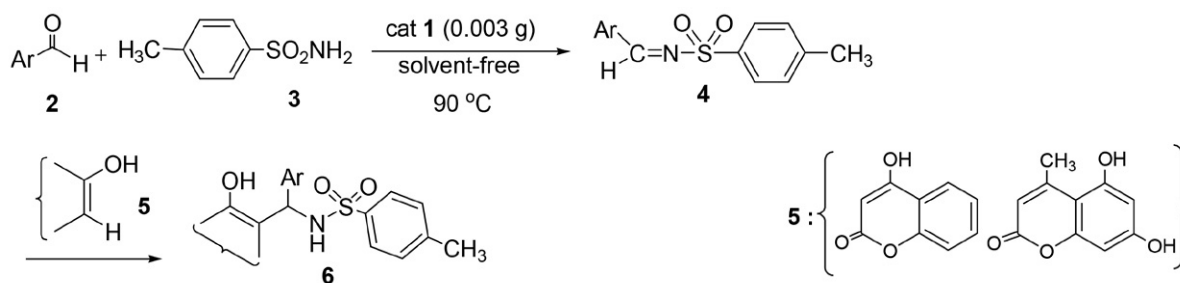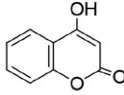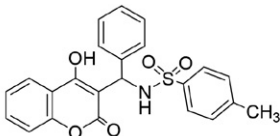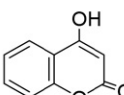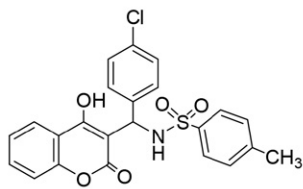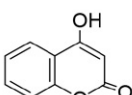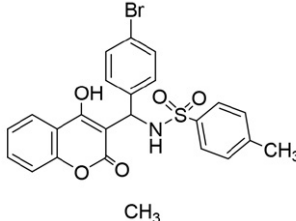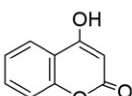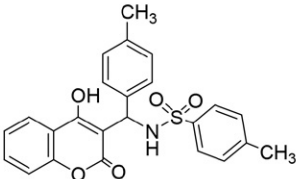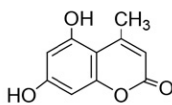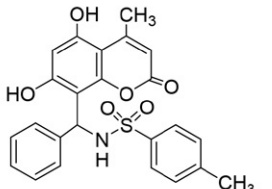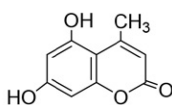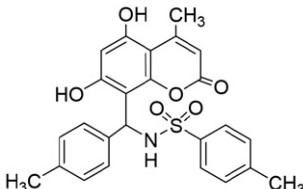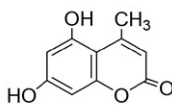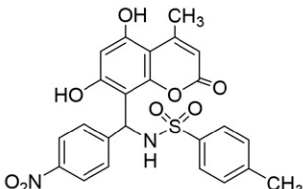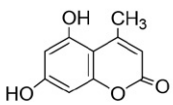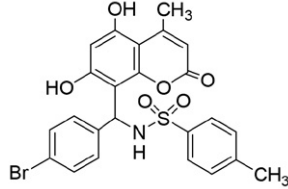

Scheme 2. Synthesis of sulfonamide containing coumarins by nanocalyst **1**.
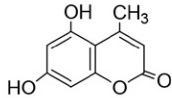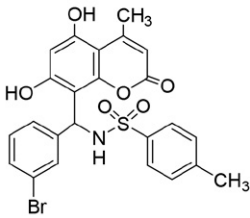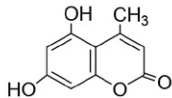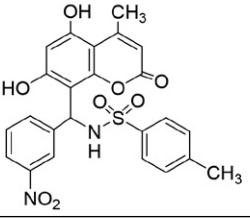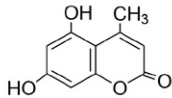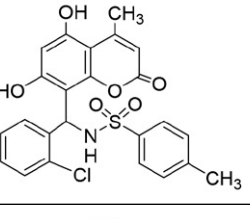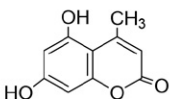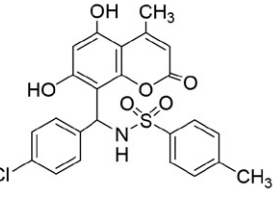
Table 1. Optimization of the model reaction.[a]

Entry	Catalyst 1 (g)	Solvent	Temp. (°C)	Time (h)	Yield[b] (%)
1	–	–	25	24	–
2	–	–	80	24	5
3	–	–	100	24	9
4	–	Toluene	reflux	24	3
5	–	EtOH	reflux	24	5
6	0.001	–	60	3	50
7	0.003	–	60	3	65
8	0.005	–	60	3	60
9	0.007	–	60	3	57
10	0.003	EtOH	reflux	3	60
11	0.003	Toluene	reflux	3	55
12	0.003	H_2O	reflux	3	48
13	0.003	$CHCl_3$	reflux	3	53
14	0.003	–	80	1.5	75
15	0.003	–	90	1.5	85
16	0.003	–	110	1.5	80

[a] Reaction conditions: benzaldehyde (1 mmol), *para*-toluenesulfonamide (1 mmol) and 4-hydroxycoumarin (1 mmol). [b] Isolated yields.

Table 2. Synthesis of **6** in the presence of $Fe_3O_4@TiO_2@(CH_2)_3OMoO_3H$.

Entry	Compound 5	Ar	Product	Mp (°C)	Time (min)
6a		C_6H_5		231–233	90
6b		$4\text{-}ClC_6H_4$		251–253	85
6c		$4\text{-}BrC_6H_4$		176–177	85
6d		$4\text{-}CH_3C_6H_4$		263–264	120
6e		C_6H_5		260–262[46]	240
6f		$4\text{-}CH_3C_6H_4$		255–256[46]	260
6g		$4\text{-}NO_2C_6H_4$		219–221[46]	200
6h		$4\text{-}BrC_6H_4$		268–269[46]	210

Entry	Compound 5	Ar	Product	Mp (°C)	Time (min)
6i		$3\text{-}BrC_6H_4$		270–271[46]	210
6j		$3\text{-}NO_2C_6H_4$		230–232[46]	200
6k		$2\text{-}ClC_6H_4$		215–216[46]	230
6l		$4\text{-}ClC_6H_4$		208-210[46]	220

^a Isolated yields.
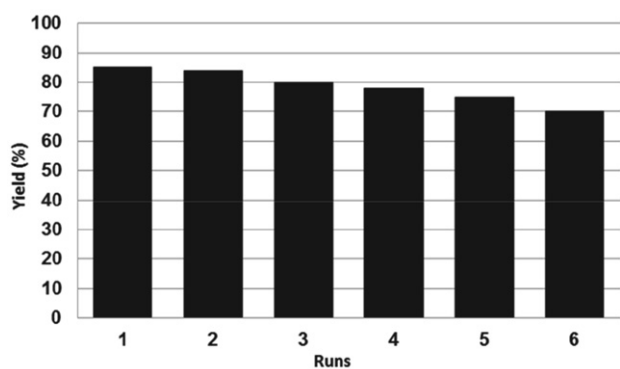
Figure 6. Reusability study of nanocatalyst **1** in the synthesis of **6a** at 90 °C under solvent-free conditions.

In a preliminary study, the reaction of benzaldehyde, *para*-toluenesulfonamide and 4-hydroxycoumarin was selected as a model reaction to determine suitable conditions. To illustrate the need of $Fe_3O_4@TiO_2@(CH_2)_3O\text{-}MoO_3H$ for this condensation, we examined the model reaction in the absence of this catalyst at various conditions. The results show clearly that $Fe_3O_4@TiO_2@(CH_2)_3OMoO_3H$ is an effective catalyst for this reaction

and in the absence of this catalyst the reaction did not take place, even after 24 h. Next, the model reaction was conducted in the presence of several amounts of catalyst **1** at different conditions (Table 1). Through screening we found that this reaction was efficiently completed in the presence of 0.003 g of $Fe_3O_4@TiO_2@(CH_2)_3OMoO_3H$ at 90 °C under solvent-free conditions.

To investigate the generality of this protocol, the reaction of different aryl aldehydes, containing both electron-donating and electron-withdrawing groups were employed in the reaction. In general, the reaction proceeded smoothly to afford the desired products **6** in good to excellent yields. Furthermore, under similar conditions, aryl aldehydes and *para*-toluenesulfonamide were reacted with 5,7-dihydroxy-4-methylcoumarin in the presence of the catalyst **1** (Table 2). According to the reported procedure in the literature,[45] 5,7-dihydroxy-4-methylcoumarin was synthesized *via* the $ZrOCl_2/SiO_2$-catalyzed condensation of phloroglucinol and ethyl acetoacetate.

Recovery and reuse of the catalysts after catalytic reactions are important factors for sustainable process management. The recovered nanomagnetic catalyst **1** from the model reaction for the synthesis of **6a** was separated by an
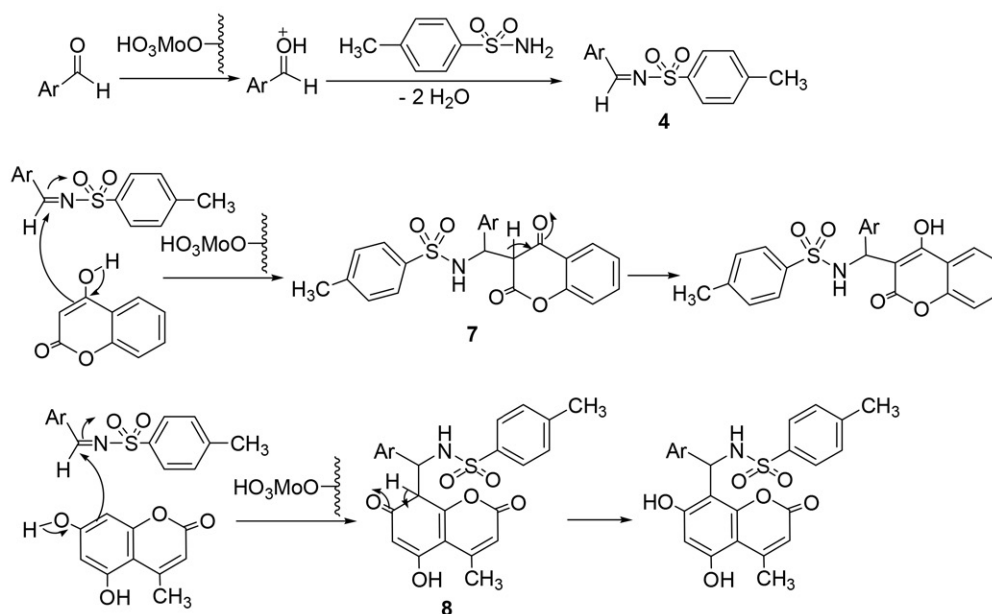
Scheme 3. Proposed mechanism for the synthesis of **6** in the presence of Fe$_3$O$_4$@TiO$_2$@(CH$_2$)$_3$OMoO$_3$H.

external magnet, washed with MeOH and reused in the next run. As outlined in Fig. 6, Fe$_3$O$_4$@TiO$_2$@(CH$_2$)$_3$O-MoO$_3$H exhibited no considerable decrease in activity after six cycles. This advantage besides the recoverability of the biodegradable and green catalyst makes this research highly favorable for large-scale synthesis.

A plausible mechanism for the synthesis of product **6** is outlined in Scheme 3. It is reasonable to assume that *para*-toluenesulfonamide attacks the activated arylaldehyde by the acid catalyst to give sulfonyl aldimines **4**. Then, intermediate **7** or **8** is generated from the condensation of **5** (5,7-dihydroxy-4-methylcoumarin or 4-hydroxycoumarin) with **4** which rearranges into the desired product.

The filtration test was performed to show the heterogeneity of the catalyst. For this purpose, after the development of about 40% of the model reaction (synthesis of **6a**), the catalyst was removed and the progress of the residual mixture was monitored. Interestingly, no further conversion was observed in this case. Therefore, we found that the catalyst operates in a heterogeneous manner and no leaching of molybdic acid as active species occurs under the applied conditions.

3. Experimental

All chemicals used in this research were purchased from Fluka and Merck chemical companies. The monitoring of the reaction progress and the purity of the compounds were accomplished using TLC performed with silica gel SIL G/UV254 plates. Melting points were determined by an electrothermal KSB1N apparatus and are uncorrected. ^{1}H NMR spectra were recorded in DMSO-d_6 on a Bruker Avance Ultra Shield 400 MHz instrument spectrometers and ^{13}C NMR spectra were recorded at 100 MHz. X-ray powder diffraction (XRD) patterns were recorded using a Bruker AXS (D8 Advance) X-ray diffractometer with Cu Kα radiation (λ = 0.15418 nm). The measurement was made in 2θ ranging from 10° to 80° at the speed of 0.05° min^{-1}. For the preparation of the sample for XRD, after synthesis, the sample was powder, which was clumpy, and then XRD was measured. Analysis conditions includes: voltage: 40 kV and current: 30 mA. Energy dispersive spectroscopy (EDS) was performed using a TESCAN Vega model instrument. The morphology of the particles was observed by scanning electron microscopy (SEM) under an acceleration voltage of 26 kV. Before SEM characterization, the sample was powdered and then coated with gold. The magnetic measurement was carried out in a vibrating sample magnetometer (VSM) at Kashan University (Kashan, Iran) at room temperature.

Synthesis of Fe$_3$O$_4$ MNPs

A solution of FeCl$_3$·6H$_2$O (1.35 g, 5 mmol) and FeCl$_2$ · 4H$_2$O (0.5 g, 2.5 mmol) (dissolved in 22 mL double distilled water) stirred under argon atmosphere at 80 °C for 30 min. Next the sodium hydroxide solution (2.5 mL, 10 M) was added dropwise to the reaction mixture with stirring for 1 h under argon atmosphere. Finally, the formed nanoparticles were collected using an external magnet. The nano particles were washed with distilled water repeatedly and then dried at 60 °C.[47]

Synthesis of nano-Fe$_3$O$_4$@TiO$_2$

Fe$_3$O$_4$ nanoparticles were added to a mixture of ethanol and acetonitrile (250:90 mL) and sonicated for 25

min. Next an aqueous ammonia solution (1.5 mL, 25 W%) was added and the resulting mixture was stirred at 25 °C for 30 min. Then, tetraethyl orthotitanate (3 mL) dissolved in absolute ethanol (20 mL) was added. After stirring for 2 h the obtained mixture was washed completely with absolute ethanol and was collected with an external magnet.[37]

Synthesis of Fe₃O₄@TiO₂@(CH₂)₃Cl

Nano-Fe₃O₄@TiO₂ (0.6 g) was added in 3-chloropropyltrimethoxysilane (6 mL) and stirred for 12 h under argon atmosphere and reflux conditions. This product was then separated *via* a magnet and washed repeatedly using toluene, ethanol-water and distilled water. Finally, Fe₃O₄@ TiO₂@(CH₂)₃Cl was dried in an oven at 60 °C.[48]

Preparation of Fe₃O₄@TiO₂@(CH₂)₃OMoO₃H

A mixture of Fe₃O₄@TiO₂@(CH₂)₃Cl (1 g) and Na₂MoO₄·2H₂O (0.5 g) in DMSO (10 mL) was stirred at reflux under argon atmosphere for 12 h. The resulting product was decanted and washed twice with DMSO, once with distilled water and was dried at 50 °C for 18 h. Then, it was added to the flask containing HCl (60 mL, 0.1 N) and stirred for 2 h at room temperature. The resulting catalyst was decanted, washed with DMSO and water, afterwards dried at room temperature.

General Procedure for the Synthesis of 6

Catalyst **1** (0.003 g) was added to the mixture of *para*-toluenesulfonamide (1 mmol), aldehyde (1 mmol) and 4-hydroxycoumarin (1 mmol) or 5,7-dihydroxy-4-methylcoumarin (1 mmol). The resulting mixture was stirred in an oil bath (90 °C) under solvent-free conditions. The reaction progress was monitored by TLC (*n*-hexane/EtOAc, 2:1). After completion of the reaction, boiling methanol (10 mL) was added, and the catalyst was separated by an external magnet. The obtained powder was recrystallized from hot EtOH.

Compound 6a: Yield: 0.357 g (85%), FT-IR (KBr) ($\bar{\nu}_{max}$, cm⁻¹): 3438, 1660, 1616, 1569, 1496, 1348, 1303, 1093, 759, 816. ¹H NMR (400 MHz, DMSO-d_6) δ (ppm): 2.51 (s, 3H), 6.39 (s, 1H), 7.15–7.19 (t, 3H), 7.23–7.27 (t, 2H), 7.33–7.40 (m, 4H), 7.60–7.64 (m, 2H), 7.92 (dd, J_1 = 9.2 Hz, J_2 = 1.2 Hz, 2H). ¹³C NMR (100 MHz, DMSO-d_6) δ (ppm): 208.8, 166.0, 153.6, 152.1, 140.5, 139, 133.5, 132.6, 131.7, 128.6, 127.1, 126.0, 124.4, 124.3, 118.0, 116.5, 104.5, 57.0, 36.4.

Compound 6b: Yield: 0.409 g (90%), FT-IR (KBr) ($\bar{\nu}_{max}$, cm⁻¹): 3438, 1668, 1616, 1562, 1494, 1438, 1351, 1311, 887, 757. ¹H NMR (400 MHz, DMSO-d_6) δ (ppm): 2.07 (s, 3H), 6.28 (s, 1H), 7.13–7.15 (d, 2H), 7.25–7.27 (d, 2H), 7.30–7.36 (m, 4H), 7.57–7.61 (m, 2H), 7.88 (dd, J_1 = 8 Hz, J_2 = 7.2 Hz, 2H), 7.92–8.5 (m, 2H). ¹³C NMR (100 MHz, DMSO-d_6) δ (ppm): 208.3, 165.7, 165.3, 153.6, 152.9, 139.4, 138.7, 132.5, 131.3, 130.3, 127.4, 124.4, 123.3, 119.0, 118.2, 116.4, 115.7, 104, 31.3.

Compound 6c: Yield: 0.773 g (84%), FT-IR (KBr) ($\bar{\nu}_{max}$, cm⁻¹): 3438, 3255, 1664, 1631, 1604, 1567, 1492, 1330, 1164, 736, 673. ¹H NMR (400 MHz, DMSO-d_6) δ (ppm): 2.31 (s, 3H), 6.32 (s, 1H), 7.16–7.37 (t, 8H), 7.57–7.61 (m, 2H), 7.89–8.10 (m, 4H). ¹³C NMR (100 MHz, DMSO-d_6) δ (ppm): 208.10, 173.16, 172.32, 162.62, 143.15, 142.42, 138.37, 129.05, 128.62, 125.37, 124.32, 122.42, 120.42, 108.15, 31.10.

Compound 6d: Yield: 0.326 g (75%), FT-IR (KBr) ($\bar{\nu}_{max}$, cm⁻¹): 3438, 1668, 1616, 1604, 1563, 1351, 1311, 1095, 736, 673. ¹H NMR (400 MHz, DMSO-d_6) δ (ppm): 2.24 (s, 3H), 2.34 (s, 3H), 6.39 (s, 1H), 7.17–7.27 (m, 3H), 7.34–7.41 (m, 8H), 7.61–7.95 (m, 3H). ¹³C NMR (100 MHz, DMSO-d_6) δ (ppm): 208.10, 173.16, 172.32, 162.62, 143.15, 142.42, 138.37, 129.05, 128.62, 125.37, 124.32, 122.42, 120.42, 108.15, 36.11, 31.10.

Compound 6k: Yield: 0.392 g (81%), FT-IR (KBr) ($\bar{\nu}_{max}$, cm⁻¹): 3471, 3338, 3170, 1673, 1610, 1575, 1413, 1157, 1091. ¹H NMR (400 MHz, DMSO-d_6) δ (ppm): 10.45 (s, 1H), 10.43 (s, 1H), 7.95 (d, 1H, J = 10.9 Hz), 7.87 (d, 1H, J = 10.0 Hz), 7.52 (d, 2H, J = 10.8 Hz), 7.28–7.08 (m, 5H), 6.20 (d, 1H, J = 10.8 Hz), 6.15 (s, 1H), 5.75 (s, 1H), 2.39 (s, 3H), 2.25 (s, 3H). ¹³C NMR (100 MHz, DMSO-d_6) δ (ppm): 159.2, 158.8, 157.2, 154.8, 153.6, 142.0, 138.8, 138.4, 131.4, 130.9, 128.9, 128.7, 128.2, 126.3, 125.9, 108.6, 103.9, 101.8, 98.5, 49.19, 23.6, 20.9.

Compound 6l: Yield: 0.412 g (85%), FT-IR (KBr) ($\bar{\nu}_{max}$, cm⁻¹): 3477, 3423, 3315, 1702, 1619, 1524, 1432, 1292, 1182. ¹H NMR (400 MHz, DMSO-d_6) δ (ppm): 10.45 (s, 1H, OH), 7.88 (d, 1H, J = 8 Hz), 7.53 (d, 2H, J = 8 Hz), 7.11–7.28 (m, 6H), 6.20 (s, 1H), 6.16 (s, 1H), 5.77 (s, 1H), 2.41 (s, 3H), 2.28 (s, 3H). ¹³C NMR (100 MHz, DMSO-d_6) δ (ppm): 159.14, 157.17, 154.73, 141.98, 138.91, 138.31, 131.33, 130.90, 129.14, 128.80, 128.66, 128.12, 126.24, 125.90, 108.64, 104.12, 98.57, 49.12, 23.54, 20.88. MS (EI): *m/z* 485 (M⁺), 301 ($C_{16}H_9ClO_4^+$), 279 ($C_{17}H_{12}O4^+$), 258 ($C_{15}H_{11}ClO_2^+$).

4. Conclusion

In summary, we have introduced Fe₃O₄@TiO₂@(CH₂)₃OMoO₃H as a novel modified Fe₃O₄ MNPs. It was fully characterized by XRD, SEM, EDS, FT-IR and VSM analysis. Furthermore, the first application of this reusable nanocatalyst for the synthesis of sulfonamide containing coumarin derivatives was successfully examined. The use of Fe₃O₄@TiO₂@(CH₂)₃OMoO₃H as a green and safe catalyst under solvent-free conditions, high yield of pure products, short reaction times and a simple recovery procedure are the main promising points of this work.

5. References

1. C. Sanchez, P. Belleville, M. Popalld, L. Nicole, *Chem. Soc. Rev.* **2011**, *40*, 696–753. **DOI:**10.1039/c0cs00136h

2. D. Zhang, X. Du, L. Shi, R. Gao, *Dalton Trans.* **2012**, *41*, 14455–14475. **DOI:**10.1039/c2dt31759a

3. M. B. Gawande, S. N. Shelke, R. Zboril, R. S. Varma, *Acc. Chem. Res.* **2014**, *47*, 1338–1348. **DOI:**10.1021/ar400309b

4. S. R. Bankar, S. Shelke, *Res. Chem. Intermed.* **2018**, *44*, 3507–3521. **DOI:**10.1007/s11164-018-3321-4

5. S. R. Bankar, *Curr. Organocataly.* **2018**, 5, 42–50. **DOI:**10.2174/2213337205666180611112941

6. M. B. Gawande, P. S.Branco, R. S. Varma, *Chem. Soc. Rev.* **2013**, *42*, 3371–3393. **DOI:**10.1039/c3cs35480f

7. S. N. Shelke, S. R. Bankar, G. R. Mhaske, S. S. Kadam, D. K. Murade, S. B. Bhorkade, A. K. Rathi, N. Bundaleski, O. M. N. D. Teodoro, R. Zboril, R. S. Varma, M. B. Gawande, *ACS Sustainable Chem. Eng.* **2014**, *2*, 1699–1706. **DOI:**10.1021/sc500160f

8. S. R. Bankar, *Curr. Organocatal.* **2019**, 6, 238–247. **DOI:**10.2174/2213337206666190415125053

9. V. Polshettiwar, R. S. Varma, *Green Chem.* **2010**, 5, 743–754. **DOI:**10.1039/b921171c

10. S. Shylesh, V. Schnemann, W. R. Thiel, *Angew. Chem. Int. Ed.* **2010**, *49*, 3428–3459. **DOI:**10.1002/anie.200905684

11. R. Hudson, Y. Feng, R. S. Varma, A. Moores, *Green Chem.* **2014**, *16*, 4493–4505. **DOI:**10.1039/C4GC00418C

12. Z. C. Zhang, B. Xu, X. Wang, *Chem. Soc. Rev.* **2014**, *43*, 7870–7886. **DOI:**10.1039/C3CS60389J

13. I. I. Slowing, J. L. V. Escoto, B. G. Trewyn, V. S. Y. Lin, *J. Mater. Chem.* **2010**, *20*, 7924–7937. **DOI:**10.1039/c0jm00554a

14. P. Das, N. Aggarwal, N. R. Guha, *Tetrahedron Lett.* **2013**, *54*, 2924–2928. **DOI:**10.1016/j.tetlet.2013.03.106

15. A. Corma, H. Garcia, *Chem. Soc. Rev.* **2008**, *37*, 2096–2126. **DOI:**10.1039/b707314n

16. B. Karimi, F. Mansouri, H. M. Mirzaei, *ChemCatChem* **2015**, *7*, 1736–1789. **DOI:**10.1002/cctc.201403057

17. M. A. Zolfigol, M. Yarie, *Appl. Organometal. Chem.* **2017**, *31*, 3598–3609.

18. T. O. Eschemann, J. H. Bitter, K. P. de Jong, *Catal. Today* **2014**, *228*, 89–95. **DOI:**10.1016/j.cattod.2013.10.041

19. H. Kominami, M. Kohno, Y. Takada, M. Inoue, T. Inui, Y. Kera, *Ind. Eng. Chem. Res.* **1999**, *38*, 3925–3931. **DOI:**10.1021/ie9901170

20. B. Kraeutler, A. J. Bard, *J. Amer. Chem. Soc.* **1978**, *100*, 4317–4318. **DOI:**10.1021/ja00481a059

21. C. Gannoun, R. Delaigle, A. Ghorbel, E. M. Gaigneaux, *Catal. Sci. Technol.* **2019**, *9*, 2344–2350. **DOI:**10.1039/C9CY00099B

22. R. Palcheva, L. Dimitrov, G. Tyuliev, A. Spojakina, K. Jiratova, *Appl. Surf. Sci.* **2013**, *265*, 309–316. **DOI:**10.1016/j.apsusc.2012.11.001

23. W. P. Kwan, B. M. Voelker, *Environ. Sci. Tech.* **2003**, *37*, 1150–1158. **DOI:**10.1021/es020874g

24. E. De Clercq, *Curr. Med. Chem.* **2001**, *8*, 1543–1572. **DOI:**10.2174/0929867013371842

25. M. Lopez, L. F. Bornaghi, A. Innocenti, D. Vullo, S. A. Charman, C. T. Supuran, S. A. Poulsen, *J. Med. Chem.* **2010**, *53*, 2913–2926. **DOI:**10.1021/jm901888x

26. J. Mun, A. A. Jabbar, N. S. Devi, S. Yin, Y. Wang, C. Tan, D. Culver, J. P. Snyder, E. G. Van Meir, M. M. Goodman, *J. Med. Chem.* **2012**, *55*, 6738–6750. **DOI:**10.1021/jm300752n

27. S. Mc Mahon, R. Kennedy, P. Duffy, J. M. Vasquez, J. G. Wall, H. Tai, W. Wang, *ACS Appl. Mater. Interfaces* **2016**, *8*, 26648–26656. **DOI:**10.1021/acsami.6b11371

28. M. Bavadi, K. Niknam, M. Gharibi, *Monatsh. Chem.* **2017**, *148*, 1025–1034. **DOI:**10.1007/s00706-016-1847-y

29. A. Cristina, S. Baetas, M. S. P. Arruda, A. H. Müller, A. C. Arruda, *J. Braz. Chem. Soc.* **1999**, *10*, 181–183. **DOI:**10.1590/S0103-50531999000300004

30. C. Spino, M. Dodier, S. Sotheeswaran, *Bioorg. Med. Chem.* **1998**, *8*, 3475–3478. **DOI:**10.1016/S0960-894X(98)00628-3

31. M. Z. Hassan, H. Osman, M. A. Ali, M. J. Ahsan, *Eur. J. Med. Chem.* **2016**, *123*, 236–255. **DOI:**10.1016/j.ejmech.2016.07.056

32. D. C. Pinto, A. M. Silva, *Curr. Top. Med. Chem.* **2017**, *17*, 3190–3198.

33. A. Lacy, R. O'Kennedy, *Curr. Pharm. Des.* **2004**, *10*, 3797–3811. **DOI:**10.2174/1381612043382693

34. J. Etemad Gholtash, M. Farahi, *RSC Adv.* **2018**, *8*, 40962–40967. **DOI:**10.1039/C8RA06886K

35. M. Farahi, F. Tamaddon, B. Karami, S. Pasdar, *Tetrahedron Lett.* **2015**, *56*, 1887–1890. **DOI:**10.1016/j.tetlet.2015.02.105

36. M. Farahi, B. Karami, R. Keshavarz, F. Khosravian, *RSC Adv.* **2017**, *7*, 46644–46650. **DOI:**10.1039/C7RA08253C

37. A. Amoozadeh, S. Golian, S. Rahimi, *RSC Adv.* **2015**, *5*, 45974–5982. **DOI:**10.1039/C5RA06515A

38. A. A. Elmekawy, J. B. Sweeney, D. R. Brown, *Catal. Sci. Technol.* **2015**, *5*, 690–696. **DOI:**10.1039/C4CY00970C

39. H. Yin, Y. Wada, T. Kitamura, S. Kambe, S. Murasawa, H. Mori, T. Sakatac, S. Yanagida, *J. Mater. Chem.* **2001**, *11*, 1694–1703. **DOI:**10.1039/b008974p

40. F. Nemati, M. Heravi, A. Elhampour, *RSC Adv.* **2015**, *5*, 45775–45784. **DOI:**10.1039/C5RA06810J

41. F. Khosravian, B. Karami, M. Farahi, *New J. Chem.* **2017**, *41*, 11584–11590. **DOI:**10.1039/C7NJ02390A

42. T. Xin, M. Ma, H. Zhang, J. Gu, S. Wang, M. Liu, Q. Zhang, *Appl. Surf. Sci.* **2014**, *288*, 51–59. **DOI:**10.1016/j.apsusc.2013.09.108

43. N. Divsalar, N. Monadi, M. Tajbaksh, *J. Nanostruct.* **2016**, *6*, 312–321.

44. B. Karami, M. Kiani, *Monatsh. Chem.* **2016**, *147*, 1117–1124. **DOI:**10.1007/s00706-015-1551-3

45. B. Karami, M. Kiani, *Catal. Commun.* **2011**, *14*, 62–67. **DOI:**10.1016/j.catcom.2011.07.002

46. M. Farahi, B. Karami, H. Mohamadi Tanuraghaj, *Tetrahedron Lett.* **2015**, *56*, 1833–1836. **DOI:**10.1016/j.tetlet.2015.02.087

47. M. C. Mascolo, Y. Pei, T. A. Ring, *Materials* **2013**, *6*, 5549–5567. **DOI:**10.3390/ma6125549

48. A. A. Elmekawy, J. B. Sweeney, D. R. Brown, *Catal. Sci. Technol.* **2015**, *5*, 690–696. **DOI:**10.1039/C4CY00970C

Povzetek

Uspešno smo pripravili molibdensko kislino imobilizirano na nano-Fe$_3$O$_4$@TiO$_2$ (Fe$_3$O$_4$@TiO$_2$@(CH$_2$)$_3$OMoO$_3$H), jo karakterizirali in uporabili kot katalizator za sintezo sulfonamidov, vsebujočih kumarinski fragment. Pripravi Fe$_3$O$_4$ nanodelcev s so-obarjanjem Fe^{2+} in Fe^{3+} ionov je sledila obdelava s tetraetil ortotitanatom, ki je vodila do nastanka Fe$_3$O$_4$@TiO$_2$. Tako dobljene delce smo nato obdelali s 3-kloropropiltrietoksisilanom, nato pa reagirali še z molibdensko kislino ter dobili željeni katalizator, ki smo ga karakterizirali z XRD, SEM, EDS, FT-IR in VSM analizami. Fe$_3$O$_4$@TiO$_2$@(CH$_2$)$_3$OMoO$_3$H smo uporabili kot katalizator za sintezo sulfonamidov, vsebujočih kumarinski fragment, ki smo jo izvedli v obliki trokomponentne reakcije med aril aldehidi, *para*-toluensulfonamidom in 4-hidroksikumarinom (ali 5,7-dihidroksi-4-metilkumarinom). Izolacija katalizatorja po končani reakciji in njegova ponovna uporaba ni pokazala nobene izgube njegove aktivnosti.